Journal of Sensor Science and Technology
Vol. 32, No. 5 (2023) pp. 280-284
http://dx.doi.org/10.46670/JSST.2023.32.5.280
pISSN 1225-5475/eISSN 2093-7563

Facile Fabrication of Micro-scale Photomask and Microfluidic Channel Mold for Sensor Applications Using a Heat-shrink Polymer

Sung-Youp Lee[1], Kiwon Yang[1], Jong-Goo Bhak[1], and Young-Soo Sohn[2,+]

Abstract

In this study, a prototype micro-scale photomask and microfluidic channel mold were fabricated using the thermal shrinkage of the polymer. A polystyrene (PS) sheet was used as the heat-shrink polymer, and the patterns of the photomask and microchannel are interdigitated electrodes. Patterns were formed on the PS sheets using a commercial laser printer. The contraction ratio of the PS sheet was approximately 60% at a temperature of 150 °C, and the transmittance was reduced by approximately 0% at a wavelength of 365 nm. The microfluidic channel had a round shape. The proposed technique is simple, facile, and inexpensive for fabricating a micro-scale photomask and microfluidic channel mold and does not involve the use of any harmful materials. Thus, this technique is well-suited for fabricating diverse micro-scale patterns and channels for prototype devices, including sensors.

Keywords: Heat-shrink polymer, Microfluidic, Photomask, Polystyrene

1. INTRODUCTION

Our daily lives are changing with convenience owing to the development of microelectronics. Advancements in fabrication techniques have facilitated the manufacture of cost-effective microelectronic devices. Automation is also an important technology that brings convenience to daily life. Microsensors are indispensable elements in the field of automation. Various fabrication techniques, including micro/nano electro-mechanical systems (M/NEMS), have been developed for microelectronics and microsensors [1-4].

The fabrication technology for M/NEMS is widely utilized for various transducers, including microsensors and microactuators [4]. Fabrication techniques, such as photolithography using ultraviolet light and scanning beam lithography using electrons, X-rays, and ion beams, are essential for fabricating micro/nano-scale devices [5]. Among the fabrication techniques for microelectronic devices, the photolithography process is known to be the costliest. The development of an appropriate optical mask is a crucial aspect in the field of lithography, which incurs substantial costs. The use of expensive masks for prototype devices is not economically feasible, and a simpler and cheaper method for fabricating micro-scale photomasks is required to develop microsensors and microelectronic devices. One alternative for addressing these challenges is the use of heat-shrinkable polymer films [6]. Thermoset polymer films have biaxially stretched and biaxially oriented properties, and when a temperature of 100 to 150 °C is applied to the thermoset polymer film, shrinkage occurs in the plane direction [2,7]. Using this property, the desired pattern can be formed on a heat-shrinkable polymer, and micro-scale patterns can then be obtained through shrinkage. Micro-patterns made using heat-shrinkable polymers can be used as optical masks in lithography. They can also be applied as micro-patterned stamps using elastomers such as polydimethylsiloxane (PDMS) [5,8]. In addition, the patterns formed by the shrinkage process have micro-scale dimensions, which are likely to be applied to microfluidic devices [9]. Additionally, if a simple and cost-effective technology is developed to produce micro-patterns, it will benefit laboratories and small industrial companies in the production of various prototype parts and devices.

This study presents a facile and inexpensive method for forming micro-scale patterns using heat-shrinkable polystyrene (PS) sheets. A milli-scale pattern was printed on a PS sheet using a

[1]Department of Physics, Kyungpook National Unversity
80 Daehak-ro, Buk-gu, Daegu 41566, Republic of Korea
[2]Biomedical Engineering, Daegu Catholic Unversity
13-13 Hayang-ro, Hayang-eup, Gyeongbuk 38439, Republic of Korea
[+]Corresponding author: sohnys@cu.ac.kr
(Received: Sep. 8, 2023, Revised: Sep. 15, 2023, Accepted: Sep. 25, 2023)

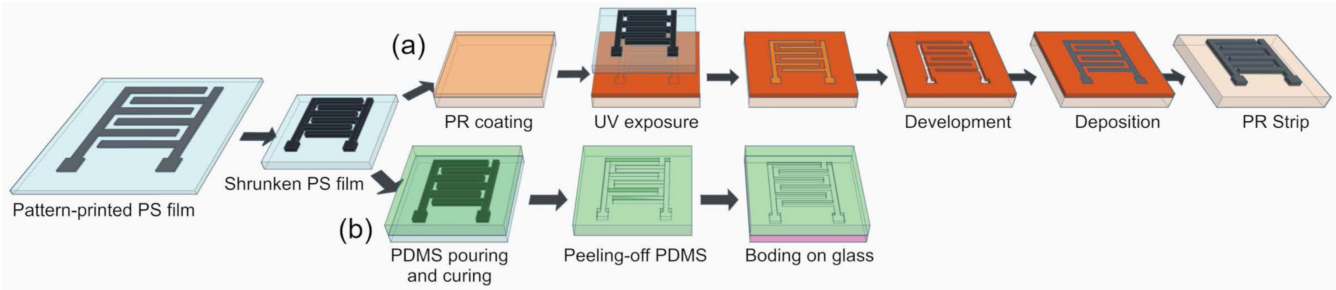

Fig. 1. Schematic illustrations for micro-scaled pattern formations using a heat shrink polymer: (a) usage of photomask, and (b) micro-channel mold for microfluidic devices.

common laser printer, and then a micro-scale pattern was subsequently subjected to a heat shrinkage process of the sheet. The structural and optical characteristics of the micro-pattern were evaluated, and its potential use as a photomask was confirmed. Additionally, the feasibility of manufacturing microfluidic devices was investigated.

2. EXPERIMENTAL

PS sheet (SizzixTM, thickness: 250 μm) was used as a heat shrink polymer, and the tested pattern on the polymer sheet was an interdigitated-electrode (IDE), which was designed using a popular office software (Microsoft PowerPoint). The patterns were printed on the sheets using a commercial laser printer (Canon, imageCLASS MF8584Cdw). The line width of the pattern ranged from 0.1 pt (35 μm) to 3 pt (1000 μm). As-printed polymer sheets were thermally treated in a furnace, and the treatment was performed at a temperature of 150 ^{o}C for 120 s. After heat treatment, the shrunken polymer may exhibit a slight curvature; in this case, a flat tool may be used to meticulously restore the polymer to a straightened state. The produced photomask can be used directly to form electrodes, as shown in Fig. 1(a). The production of the microfluidic channel mold proceeded through the following processes: PDMS (Dow Corning, SILGARD 184) was used to form the channels of the microfluidic device. The base material and hardener were mixed at 7:1, and air bubbles in the mixed solution were removed under vacuum (5×10^{-3} Torr) for 10 min. The patterned mask was placed in a glass Petri dish, and the mixed solution was poured. Subsequently, it was cured at a temperature of 100 ℃ for one hour. Fig. 1(b) illustrates the fabrication procedure for the microchannels using PDMS.

The optical transmittance of the pattern-printed sheets was investigated using a UV-Vis spectrometer (Shimadzu, UV-1280). The optical properties of the pattern on the PS sheet were analyzed using a UV lamp (Unitec, LF-215L, 365 nm, 2 × 15 W) and an optical emission spectrometer (Ocean Optics, USB2000). The pattern width and height were measured using scanning electron microscope (SEM, Hitachi, S-4800) and a digital microscope camera (Amscope, MU1000).

3. RESULTS AND DISCUSSIONS

Fig. 2 shows the change in the width of the printed line before and after the heat treatment of the PS. Lines printed at 0.1 and 0.5 pts were excluded from the device fabrication because the printed patterns on the PS sheet were not clear and continuous. The line widths corresponding to 1.0, 1.5, 2.0, 2.5, and 3.0 pts were measured to be 306, 482, 619, 835, and 1010 μm, respectively. After the heat treatment, the line widths were 163, 211, 270, 350, and 409 μm, respectively, and the shrinkage rate was almost constant. The shrinkage rate (*SR*) can be expressed as the ratio of the reduced length to the original length, and the *SR* is given by

$$SR = \frac{d_0 - d}{d_0} \quad (1)$$

where d_0 is the original length, and d is the reduced length. The calculated shrinkage rate was approximately 55 – 60% after heat treatment. In addition, the clarity of the pattern was enhanced by the contraction of the PS sheet, as shown in Fig. 2(b).

The spacing between electrodes in the IDE is 2 mm from the center-to-center. Fig. 3(a) shows the IDE patterns before and after the shrinkage process, which become more apparent after the shrinkage process. Generally, the toner for laser printers consists of microplastic powder, silica, and various inorganic materials such as iron, chromium, and zinc. However, the composition of

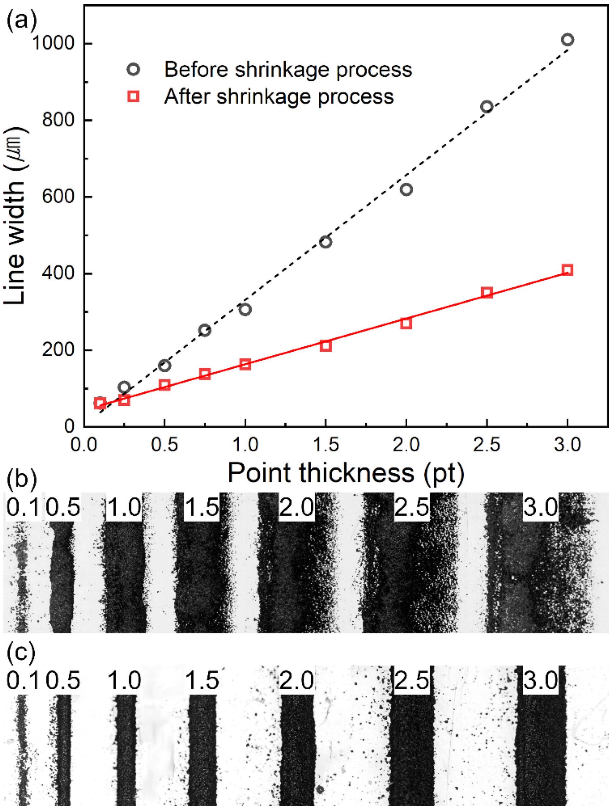

Fig. 2. (a) The variations of the line width before and after the shrinkage process of the line-printed PS sheet according to the line thickness, (b) photographs of line pattern printed on the PS sheet before and (c) after the shrinkage process. The line widths corresponding to 1.0, 1.5, 2.0, 2.5, and 3.0 pts were measured to be 306, 482, 619, 835, and 1010 μm, respectively.

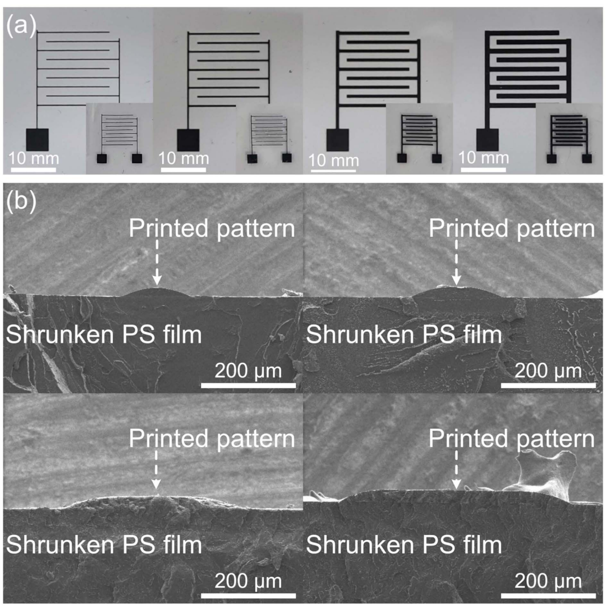

Fig. 3. (a) Photographs of IDE patterns before and after the shrinkage process and (b) cross-sectional SEM image of the patterns after the shrinkage process.

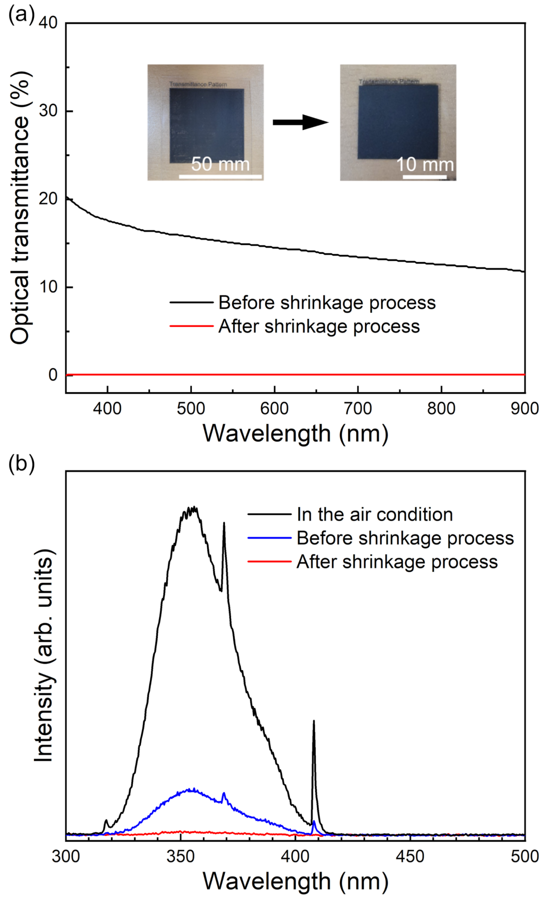

Fig. 4. (a) The transmittance and (b) the optical emission spectra of the printed PS sheet before and after the shrinkage process.

the toner varied between various companies. During shrinkage, the printed toner component of the polymer softens. The height of the pattern increased from 10 μm to 25 μm as concomitant with the shrinking of the polymer sheet. Defects, such as cracks, were not observed in the contracted patterns, and the pattern edge exhibited a soft curvature toward its termination. The cross-sectional images of the shrunken patterns on the PS sheets are shown in Fig. 3(b).

The increased pattern thickness is closely related to the transmittance of light. In photolithography, light transmission through a photomask plays a crucial role in determining the pattern quality. Fig. 4 (a) shows the transmittance of the printed pattern region before and after the shrinkage process of the PS sheet using a UV-Vis spectrometer. The transmittance before film shrinkage was 15.1% at a wavelength of 500 nm and reduced to approximately 0% after film shrinkage. Fig. 4(b) shows the optical emission spectra of the light intensities of the patterns printed on the film before and after the shrinkage process. Here, the transmittance is calculated from the optical emission spectra. The

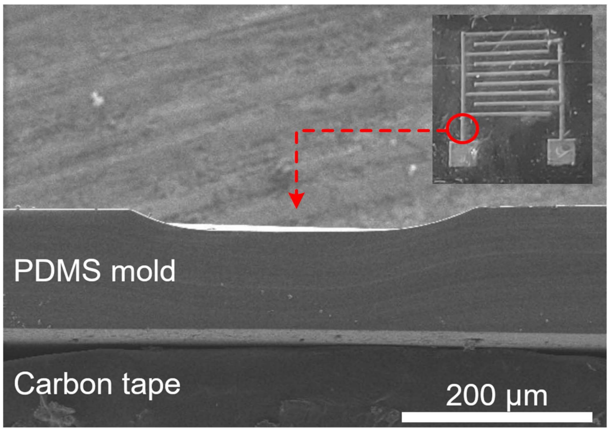

Fig. 5. The cross-sectional SEM image of PDMS micro-channel (inset: photographic image of PDMS microfluidic mold with an interdigitated electrode pattern)

transmittance before film contraction was 14.2%, and the transmittance after the shrinkage process was approximately 0% at a wavelength of 365 nm. When the printed pattern contracted during the shrinkage process of the PS sheet, the density of the pattern increased, and the ability to block light through the pattern was enhanced. Thus, the as-formed photomask exhibits suitable properties for the micro-scale lithographic processes.

Fig. 5 shows a cross-sectional SEM image of the PDMS microchannel. It has a round shape with a smooth surface, similar to the patterned structure on the shrunken PS sheet. The flow characteristics are contingent upon the roughness of the microchannel. This could affect the flow rate, velocity, and pressure, thereby interfering with the steady fluid flow along the microchannel. Therefore, the smooth surface of the microchannel contributed to a consistent fluid flow. In addition, the corners of the as-formed microchannel were round, which enhanced the fluid flow consistency. Generally, the flow efficiency of a fluid is superior in a circular cross-section compared to a rectangular shape. Thus, microchannels with round structural corners are expected to have the advantage of consistent fluid flow along the microchannel.

4. CONCLUSIONS

In this study, we fabricated a micro-scale pattern on a heat-shrinkable PS sheet for application as a micro-scale photomask and microfluidic mold for the channel. The interdigitated electrode pattern was designed using Microsoft Office software and printed on a PS sheet using a commercially available laser printer. As the PS sheet shrank, the pattern contracted at a shrinkage rate of 55-60%. During the shrinkage process, the optical transmittance of the printed region decreased from 14.2 % to approximately 0% at 365 nm. These results demonstrated that it can be applied as a photomask in photolithography. A microfluidic channel was formed using PDMS on this pattern. The microfluidic channel was round, preventing irregular flow and enhancing the flow efficiency. The process proposed in this study is a suitable technology that can fabricate micro-scale photomasks or microfluidic molds in various shapes for channels cost-effectively and quickly. Additionally, it may serve as a fabrication technique to fabricate various prototype sensors.

ACKNOWLEDGMENT

This research was supported by the Basic Science Research Program through the National Research Foundation of Korea (NRF) funded by the Ministry of Education (NRF-2019R1I1A1A01059259).

REFERENCES

[1] T. Arakawa, D. V. Dao, and K. Mitsubayashi, "Biosensors and chemical sensors for healthcare monitoring: A review", *IEEJ Trans. Electr. Electron. Eng.*, Vol. 17, No. 5, pp. 626-636, 2022.

[2] Y. Zhang, J. Liu, H. Wang, and Y. Fan, "PDMS-based microfluidic devices with shrinkable wax molds printed on biaxially orientated polystyrene film", *Mater. Res. Express*, Vol 6, No. 7, pp. 075329(1)- 075329(7), 2019.

[3] A. C. Roy, S. B. Subramanya, S. M. Rudresh, and V. Venkataraman, "On chip optofluidic low-pressure monitoring device", *J. Biophotonics*, Vol. 14, No. 3, pp. e202000381(1)-e202000381(13), 2020.

[4] W. He, X. Ye, and T. Cuit, "Progress of shrink polymer micro-and nanomanufacturing", *Microsyst. Nanoeng.*, Vol. 7, pp. 88(1)-88(23), 2021.

[5] S. Dwivedi, *"Fabrication Techniques and Materials for Bio -MEMS," in MEMS and Microfluidics in Healthcare*, K. Guha, G. Dutta, A. Biswas, and K. S. Rao, Eds. Springer, Singapore, pp. 101-141, 2023.

[6] X. Song, D. Fu, S. Shah, and J. Reif, "UV-micropatterned miniaturization: rapid in situ photopatterning and miniaturization of microscale features on shrinkable thermoplastics", *Adv. Mater. Technol.*, Vol. 5, No. 6, pp. 2000146(1)-200146(7), 2020.

[7] M. R. A. Fuaad, M. N. Hasan, M. I. A. Asri, and M. S. M. Ali, "Microactuators technologies for biomedical applications", *Microsyst. Technol.*, Vol. 29, pp. 953-984, 2023.

[8] M. Humood, J. Lefebvre, Y. Shi, M. Han, C. D. Fincher, M.

Pharr, J. A. Rogers, and A. A. Polycarpou, “Fabrication and Mechanical Cycling of Polymer Microscale Architectures for 3D MEMS Sensors”, *Adv. Eng. Mater.*, Vol. 21, No. 3, pp. 1801254(1)-1801254(10), 2019.

[9] G. G. Morbioli, N. C. Speller, and A. M. Stockton, “A practical guide to rapid-prototyping of PDMS-based microfluidic devices: A tutorial”, *Anal. Chim. Acta*, Vol. 1135, pp. 150-174, 2020.